HETEROCYCLES, Vol. 102, No. 2, 2021, pp. 231 - 244. © 2021 The Japan Institute of Heterocyclic Chemistry
Received, 7th September, 2020, Accepted, 11th December, 2020, Published online, 21st December, 2020
DOI: 10.3987/COM-20-14366

SYNTHESIS OF POLY(CYCLOTRIPHOSPHAZENE-*CO*-3,3'-SULFONYLDIANILIDE) MICROSPHERES AND THEIR ADSORPTION OF ANIONIC (CONGO RED) DYE

Zeng Xiong, Yanfei Wang,* Xiaoqing Xie, Honzheng Li, and Chen Yao

School of Chemistry and Chemical Engineering, University of South China, Hengyang, Hunan 421001 PR China; Corresponding author E-mail addresses: wyf_hn@hotmail.com

Abstract – The cyclomatrix phosphazenes-*co*-3,3'-sulfonyldianiline PSD-NH_2 microspheres with active amino groups on the surface were prepared by precipitation which was used to removal organic dyes from aqueous solution. The synthesized amino cyclomatrix phosphazenes (PSD-NH_2) microspheres were characterized by FT-IR, SEM, XPS and XRD. The effects of different pH, sorbent dosage, contact time, initial Congo red (CR) concentration and different temperature on the adsorption of Congo red by the cross-linked microspheres were studied. The experimental data show that the adsorption capacity of PSD-NH_2 microspheres on Congo red reaches 186.70 mg/g under the optimal adsorption conditions. It conforms to the pseudo-second-order kinetic equation and Langmuir isotherm model. The selective adsorption mechanism for Congo red dye can be summarized as intermolecular electrostatic interaction, hydrogen bond between PSD-NH_2 microspheres adsorbed on the surface and Congo red, π-π and C-H…π stacking and other molecular forces. Thermodynamic studies have shown that the adsorption of Congo redon PSD-NH_2 microspheres is endothermic and spontaneous in nature. Thus, amino polyphosphazene (PSD-NH_2) microspheres have excellent adsorptionperformance for Congo red.

INTRODUCTION

In this day and age, the industrial wastewater produced and discharged by plastics, printing, prevention, papermaking, electroplating and other industries contains a large amount of toxic azo dyes and heavy metal ions, which are easy to accumulate in the ecological environment due to their poor biodegradability, thus causing great harm to human health and ecological environment.[1-3] Organic compounds have widely

in the dye, paper, textile and other industrial fields.[4] However, the highly water-soluble Congo red has a high loss rate during the production and use process, which easily enters the water body and has difficulty to degrade, and even it can transform into carcinogenic and toxic aromatic amines under anaerobic conditions, which is harmful to the environment, aquatic organisms and human health.[5-7] At present, the commonly used methods for treating dye wastewater include adsorption,[8] condensation,[9] photocatalytic degradation,[10,11] biodegradation and so on.[12] Commonly used organic dye adsorbents are mainly various types of porous materials with high specific surface area, such as activated carbon,[13] zeolite,[14] clays,[15] porous metal oxides,[15] carbon-based materials,[16] chitosan[17] and composite materials etc.[18,19]

For the past few years, the use of polymer nanomaterials for dye adsorption has received extensive attention from researchers. The main reason is that these nanomaterials not only have more active sites to adsorb dyes, but we can also control their surface functional groups and internal structure, etc. Such as polydopamine materials,[20] polypyrrole-based composite materials,[21] polyurethane materials,[22] porous polyurea[23] and other polymer materials as adsorbents to remove dyes have achieved good results. In addition, polyphosphazene base materials are functional materials.[24] The side chain substituents are determined by the selected comonomers, so this type of material has a strong designability.[25] By adjusting the polymerization reaction conditions,[25] it is possible to synthesize polyphosphazene materials with different morphologies. This led us to develop a new type of adsorbent-amino polyphosphazene material.

In this experiment, amino polyphosphazene microspheres were prepared by one-step precipitation polymerization.[26] By using hexachlorocyclotriphosphazene (HCCP) and 3,3'-sulfonyldianiline as the comonomer and triethylamine as the acid binding agent, precipitation polymerization takes place under mild conditions. In this paper, the effects of different experimental conditions such as the equilibrium time, the amount of adsorbent, the initial concentration of dye and the isotherm model (Langmuir, Freundlich) and analyzes the thermodynamics and kinetics of PSD-NH_2 adsorption of Congo red, and studies the PSD-NH_2 micro mechanism of ball removal of dye.

RESULTS AND DISCUSSION

In this experiment, hexachlorocyclotriphosphazene (HCCP) and 3,3'-sulfonyldianiline were used to synthesize an amino-containing polymer through one-step precipitation polymerization. The microsphere is used to adsorb Congo red dye in the waste liquid, and its characteristics and stability are studied by FT-IR, XPS, SEM, etc. Evaluate its application in removing dyes from wastewater. The experimental data show that when pH=3.5, adsorption time is 120 min, mass is 5 mg, and the initial concentration of Congo red is 120 mg/L, the optimal adsorption capacity of Congo red is 186.70 mg/g. At the same time, according to the experimental parameters of adsorption isotherms and kinetics, the results show that the

adsorption process live up to the Langmuir isotherm adsorption model (showing single-layer adsorption) and the pseudo-second-order kinetic model (chemisorption process). Thermodynamic experiments show that the adsorption behavior of Congo red on the PSD-NH_2 is an endothermic and spontaneous process.

Characterization of poly(cyclotriphosphazene-*co*-3,3'-sulfonyldianiline). Figure 1 shows the FT-IR of monomer hexachlorocyclotriphosphazene, 3,3-sulfonyldianiline and PSD-NH_2 microspheres. The absorption bands at 3393-3451 cm^{-1} is the stretching vibration absorption bands of –NH_2 which indicates that the polymerized PSD-NH_2 microspheres contain a certain amount of –NH_2 groups.[27] The strong absorption peaks of 1600 and 1470 cm^{-1} correspond to C=C in aromatics, 1300 m^{-1} and 1150 cm^{-1} are the characteristic absorption peaks of O=S=O telescoping vibration of the sulfonic diphenol group, the absorption peak of P=N at 1211 cm^{-1} and the stretching vibration peak of Ar-N-P at 958 cm^{-1},[28,29] due to the formation of Ar-N-P it can be preliminarily inferred that hexachlorocyclotriphosphazene and 3,3'-sulfonyldianiline have precipitated and polymerized to form new substances.[30] The XPS spectrum of the PSD-NH_2 microspheres is shown in Figure 1d, which indicates the presence of O, N, C, S ,Cl and P elements in this microspheres and the weight ratios are 13.0%, 17.0%, 52.6%, 5.3%, 2.6% and 9.5% which in line with the theoretical values of ring cross-linked microspheres, thus indicating that PSD-NH_2 microspheres have been successfully prepared.

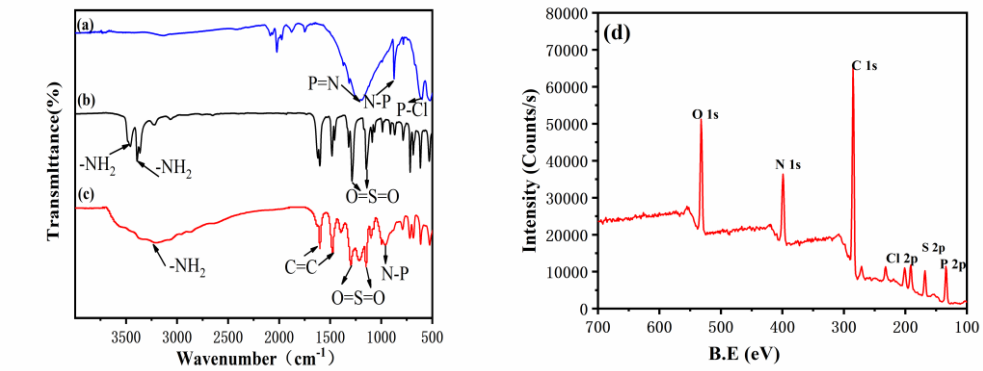

Figure 1. FTIR spectra of different monomers: (a) hecachlorocyclotriphosphazene (HCCP). (b) 3,3'-sulfonyldianiline, and (c) PSD-NH_2 microspheres. (d) XPS Spectrum of PSD-NH_2 microspheres

It can be seen from Figure 2a that the material exhibits a regular and relatively uniform spherical shape. Figure 2b shows that the adsorbed microspheres show a rough spherical structure. XRD was used to characterize the synthesized poly(cyclotriphosphazene-*co*-3,3'-sulfonyldianilide) PSD-NH_2 microspheres and their changes after adsorption of Congo red. The XRD spectrum is shown in Figure 2c. The characteristic diffraction peak appears in the range of 22.02°, indicating that there is a local layer spacing of the (sulfonyl)diimide layers in the microspheres, and the appearance is a ring-crosslinked amorphous structure.[31] After mixing with the aqueous solution containing Congo red, it was found that the

characteristic diffraction peak became stronger, indicating that the molecular structure didn't change after the dye was adsorbed.

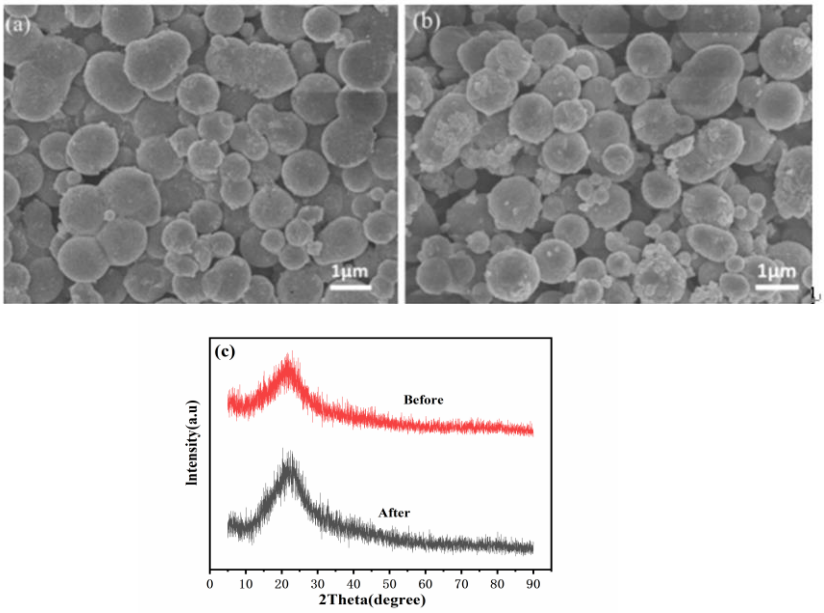

Figure 2. (a) and (b) respectively correspond to the SEM before and after PSD-NH_2 adsorption of Congo red solution. (c) XRD patterns of before and after loaded with Congo red

Effect of pH. Accurately 10 mL (120 mg/L) Congo red aqueous solution with different pH conditions (2.0, 2.5, 3.0, 3.5, 4.0, 4.5, 5.0, 5.5) were added to an Erlenmeyer flask, and 5 mg PSD-NH_2 microspheres were added under ultrasonic dispersion. The mixture was dispersed at a shaking rate of 120 rpm and room temperature (30 °C) for 2 h. After centrifuge (4000 rpm) for solid-liquid separation, a WF-J2100 was used to measure Congo red concentrations in the filtrate. The adsorption capacity (Q, mg/g) and removal rate (R,%) of Congo red were calculated according to equations(1) and (2):[32]

$$Q(mg/g) = \frac{(C_0 - C_e)V}{m} \quad (1)$$

$$R(\%) = \frac{(C_0 - C_e)100}{C_0} \quad (2)$$

Where C_0 is the initial concentration of Congo red (mg L^{-1}); C_e the concentration after adsorption (mg L^{-1}); V is the solution volume (L) and m is the quantity of PSD-NH_2 (mg).

The pH value of the solution will affect the surface charge, space structure, adsorption site and the performance of the solution.[33] It can be seen from Figure 3 that when the pH value between 2.0 and 3.5, the adsorption reaches the maximum value (the adsorption capacity is 179.18 mg/g). This is mainly due to the anionic dyes being positively charged on the surface by protonation of the adsorbent under strong acid conditions. These positively charged hydrogen ions combine with the adsorption sites in the PSD-NH_2 microspheres, thereby obtaining a good adsorption effect through the electrostatic adsorption of dye

molecules. Simultaneously, as the pH value of the solution increases, the amino groups on the surface of the adsorbent will protonate and become negatively charged, and a mass of hydroxide ions will compete with the dye ions to generate electrostatic repulsion, which is consistent with the trend reported in the literature.[34,35] The experimental results show that adsorption is favorable under acidic conditions, but considering the actual situation the greater the acidity, the higher the requirements for equipment and the stronger the corrosiveness. Therefore, the optimum adsorption condition is pH 3.5.

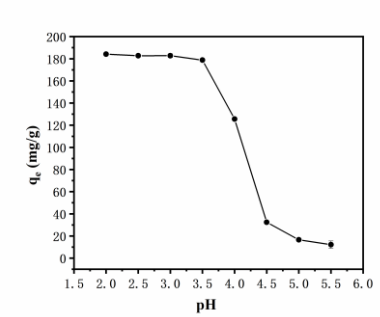

Figure 3. The effect of pH on adsorption of Congo red by PSD-NH_2 microspheres, (PSD-NH_2 dosage of 5 mg, the concentration of 120 mg/L, time of 120 min, temperature of 313 K and volume 10 mL)

Effect of adsorbent dosage. The experiment was used different adsorbent masses (3- 8 mg) under the constant condition of Congo red solution (10 mL, 120 mg/L), time of 120 minutes, pH of 3.5. The adsorption effect of the adsorbent on the Congo red solution is shown in Figure 4. The removal rate of Congo red escalate with the increase of the adsorbent. This is because the number of adsorbed active sites increase with the increases of the adsorbent, thereby improving the adsorption effect. That, under a certain concentration of adsorbate, the addition amount of adsorbent is too small, the adsorption is incomplete, and the removal rate is low; if the amount is too much, there are too many adsorption sites on the adsorbent surface of the adsorbent, and the adsorption can not reach saturation low capacity. Therefore, considering the relationship between the removal rate and the adsorption capacity, 5 mg of PSD-NH_2 was selected as the optimal adsorbent dosage.

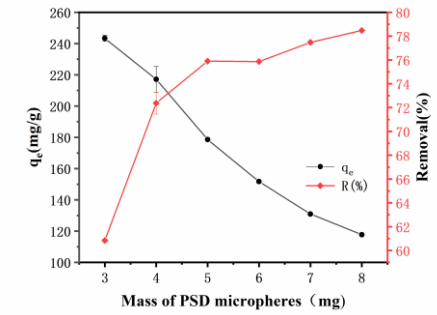

Figure 4. The effect of the amount of adsorbent on the adsorption of Congo red by PSD-NH_2 (The concentration of Congo red dye was 120 mg/L, pH 3.5, time of 120 min, temperature of 313 K and volume 10 mL)

Effect of initial Congo red concentration. The relationship between adsorption capacity and initial concentration is shown in Figure 5a. It can be seen from the figure that when the concentration of Congo red is 80 to 140 mg/L, the adsorption capacity increases. This is because PSD-NH_2 microspheres introduce amino groups, and the Congo red dye molecule contains anions such as sulfonate. The active groups such as amino can generate electrostatic attraction with the sulfonate of the dye molecule though physical and chemical adsorption processes. More dye molecules occupy the active sites on the surface of the adsorbent, thereby increasing the adsorption capacity. When the content of Congo red in the solution is greater than 110 mg/L, the adsorption capacity gradually slows down. This may be for the adsorption sites on the adsorbent have reached saturation after the Congo red solution reaches a certain concentration, and the adsorbent can no longer adsorb more Congo red dye.[36] Therefore, 120 mg/L was selected as the optimal adsorption condition. Figure 5b is a schematic diagram of before and after Congo red adsorption. It is obvious from the figure that the Congo red solution after adsorption becomes almost limpidity. Therefore, it shows that PSD-NH_2 microspheres are a kind of highly efficient adsorption material.

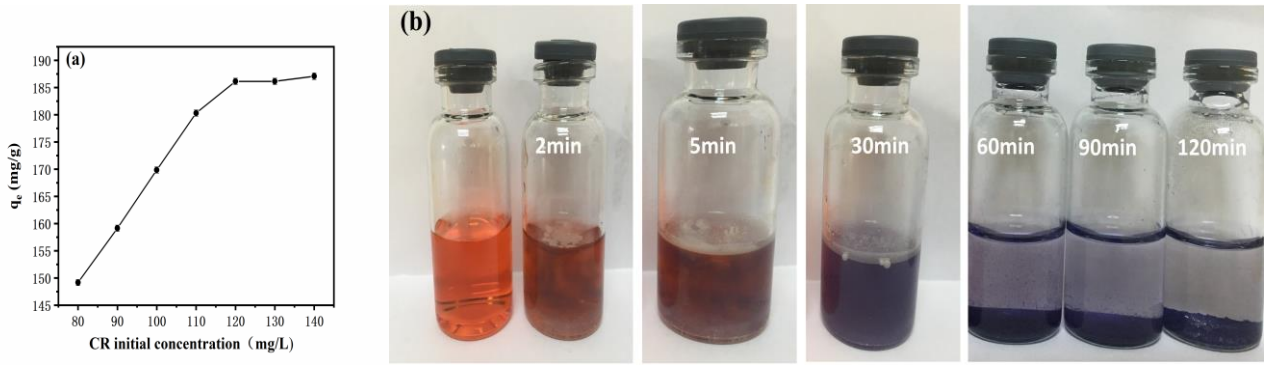

Figure 5. (a) The effect of initial concentration on adsorption of Congo red by PSD-NH_2. (b) PSD-NH_2 microspheres adsorption Congo red solution (120 mg/L) comparison chart (PSD-NH_2 dosage of 5 mg, pH 3.5, time of 120 min, temperature of 313 K and volume 10 mL)

Adsorption isotherm. In order to further explain the adsorption mechanism of Congo red by PSD-NH_2, Langmuir and Freundlich isotherm were used to fit the experimental data, which are represented by equations(3) and (4),[37] respectively:

$$\frac{C_e}{q_e} = \frac{C_e}{q_{max}} + \frac{1}{bq_{max}} \quad (3)$$

$$\ln q_e = \ln K_f + \frac{\ln C_e}{n} \quad (4)$$

Where C_e is the equilibrium concentration of Congo red in the filtrate solution (mg L^{-1}), q_e is the equilibrium adsorption capacity (mg g^{-1}), q_{max} is the maximum adsorption capacity (mg g^{-1}), b is the Langmuir adsorption equilibrium conatant (L mg^{-1}), K_f is the Freundlich adsorption conatant and 1/n is

the adsorption intensity constant.

The adsorption isotherm of PSD-NH_2 microspheres on Congo red is shown in Figure 6, and the relevant parameters calculated by the fitting equation are shown in Table 1. We found that the Langmuir isotherm model (R^2=0.9991) fits better than the Freundlish isotherm model (R^2=0.9207). By fitting the curve, and the q_{max} value (194.55 mg g^{-1}) of Langmuir isotherm model was close to the experimental q_{max} value of 186.70 mg g^{-1}, which shows that the process of adsorbing anionic dyes by our prepared amino microspheres follows the Langmuir isotherm adsorption model. The adsorption active sites on the surface of the aminocyclomatrix phosphazene microspheres are consistent and with the single-layer adsorption.[38] Its maximum adsorption capacity is higher than the maximum adsorption capacity of Congo red by bamboo hydrochars, metal oxide, composite material, solid phase adsorbent, chitosan and other adsorbents reported in the literature (Table 2)

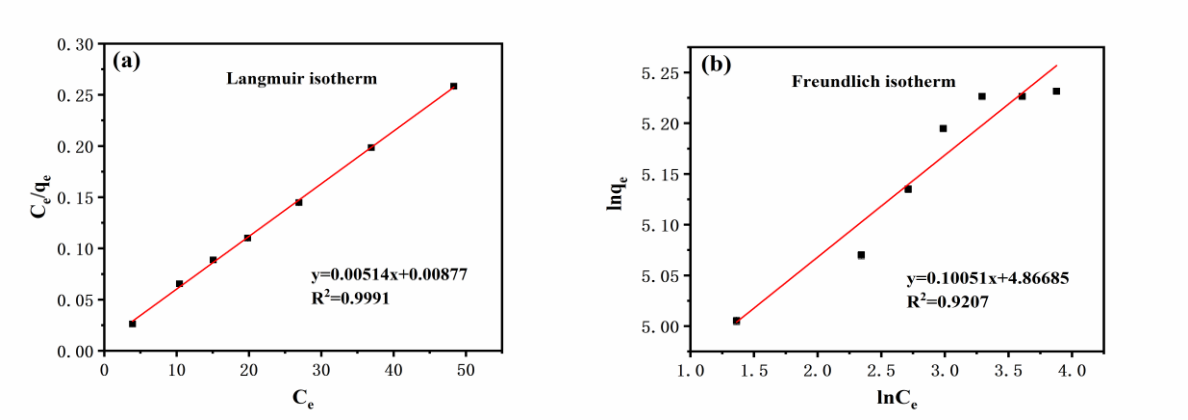

Figure 6. (a) and (b) Langmuir and Freundlich plots for the Congo red adsorption on PSD-NH_2 microspheres (The concentration of Congo red dye was 120 mg/L ,PSD-NH_2 dosage of 5 mg, pH 3.5, time of 120 min, temperature of 313 K and volume 10 mL)

Table 1

The isothermal adsorption model parameters

Isotherm	Parameters	Congo red
Langmuir	q_{max} (mg g^{-1})	194.55
	b (L g^{-1})	0.586
	R^2	0.9991
Freundlich	K_f (mg g^{-1})/(mg L^{-1})$^{1/n}$	129.91
	$\frac{1}{n}$	0.101
	R^2	0.9207

Table 2

Comparison of the maximum adsorption capacity of different adsorbents for Congo red dye

Adsorbents	Adsorption capacity（mg g^{-1}）	References
Bamboo Hydrochars	33.7	39
Mg–Al-layered double hydroxide	37.16	40
Cetyltrimethyl ammonium bromide (CTAB)	27.32	41
MWCNTs/Calcined eggshell	139.99	42
$[Zn(BDC)(TIB)]\cdot 3H_2O$ Solid-phase	60	43
Chitosan hydrobeads	92.59	44
PSD-NH_2 microspheres	186.70	This experiment

Adsorption kinetic. Through the adsorption kinetics, the effect of PSD-NH_2 microspheres on the adsorption of Congo red dye at different times was studied, as shown in Figure 7(a). The experimental results show that the adsorption capacity of Congo red reaches the maximum after 2 h of reaction, and basically remains unchanged which can be considered as adsorption equilibrium. So, 2 h is chosen as the optimum adsorption time in the following experiments. The experimental data were fitled with quasi-first-order kinetic model (5) and quasi-second-order kinetic model (6).[45,46]

$$\ln(q_e - q_t) = \ln q_e - k_1 t \quad (5)$$

$$\frac{t}{q_t} = \frac{1}{k_2 (q_e)^2} + \frac{t}{q_e} \quad (6)$$

k_1 (min^{-1}) and k_2 (g mg^{-1} min^{-1}) are the rate constant of quasi-first-order and quasi-second-order,respectively, q_e represents the adsorption capacity at equilibrium and q_t is a certain time adsorption capacity. The rate constants (k_1, k_2) and correlation coefficients obtained by linear fitting are shown in Figures 7(b) and 7(c).

As shown in Table 3, the linear fitting of the quasi-second-order kinetic (R^2=0.9979) is better than that of the quasi-first-order kinetics (R^2=0.7201), and the theoretical value of the second-order kinetic model is q_e (194.17 mg g^{-1}), it is close to the experimental value q_e (186.70 mg g^{-1}), from which we can infer that

the adsorption behavior of PSD-NH_2 microspheres on Congo red basically follows the quasi-second-order kinetic model.

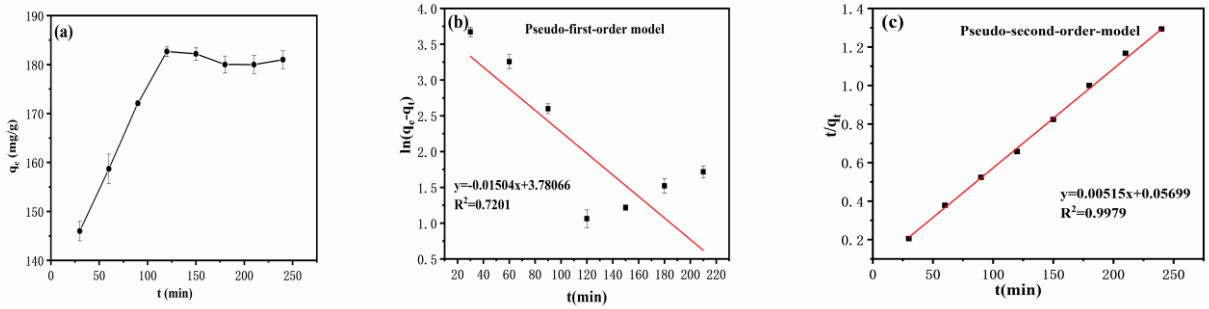

Figure 7. (a) Effect of oscillating time on the adsorption of Congo red by PSD-NH_2 microspheres. (b) and (c) pseudo-first-order kinetic and pseudo-second-order kinetic plots for the Congo red adsorption on PSD-NH_2 microspheres (the concentration of Congo red dye was 120 mg/L, PSD-NH_2 dosage of 5 mg, pH 3.5, time of 120 min, temperature of 313 K and volume 10 mL)

Table 3

Kinetic parameters of the adsorption

Pseudo-first-order	Value	Pseudo-second-order	Value
q_e (mg g^{-1})	43.84	q_e (mg g^{-1})	194.17
k_1	0.015	k_2	0.0005
R^2	0.7201	R^2	0.9979

Thermodynamics Research. To further investigate the adsorption thermodynamics of Congo red on PSD-NH_2, adsorption experiments at different temperatures (293.15-333.15K) are studied, this is shown in the following Eqs. (7), (8) and (9).

$$K_d = \frac{C_0 - C_e}{C_e} \times \frac{V}{m} \quad (7)$$

$$\ln K_d = \frac{\Delta S^0}{R} - \frac{\Delta H^0}{R \times T} \quad (8)$$

$$\Delta G^0 = \Delta H^0 - T \times \Delta S^0 \quad (9)$$

Where K_d is the equilibrium constant (mL g^{-1}), V is the solution volume (mL), m is the amount of adsorbent (mg), T is the absolute temperature in Kelvin (K) and R is the ideal gas constant (8.314 J mol^{-1} K^{-1}). The values of ΔH^0 and ΔS^0 were calculated from the slopes and intercepts of plots of Figure 8, and ΔG^0 is calculated by the formula (7), and the relevant parameters of adsorption thermodynamics are in Table 4.

Experimental data show that the adsorption capacity of PSD-NH_2 microspheres on Congo red gradually increases with temperature. It can also be said that increasing the temperature of the solution can increase the adsorption effect of PSD-NH_2 microspheres on Congo red. ΔH^0 is a positive value, the adsorption process of Congo red by PSD-NH_2 microspheres is an endothermic process, and increasing the temperature of the solution is beneficial to the adsorption reaction. ΔG^0 is negative at different temperatures, indicating that the adsorption of Congo red by PSD-NH_2 microspheres is a spontaneous process.

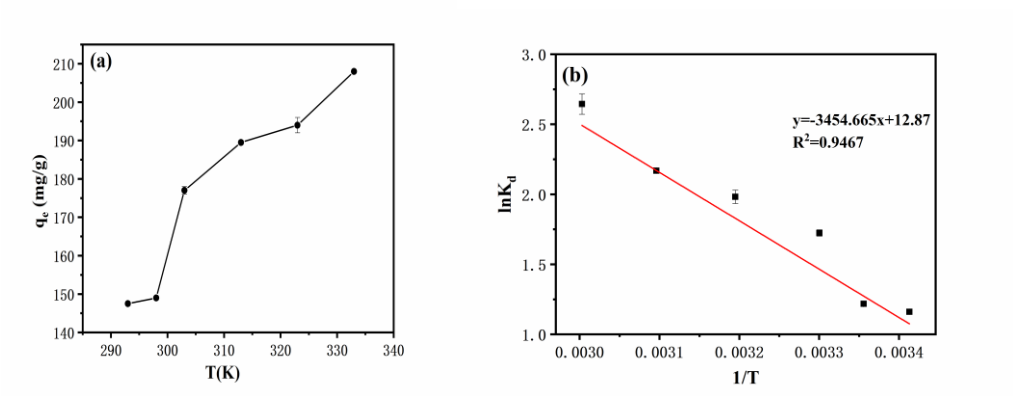

Figure 8. (a)Effect of different initial temperatures on adsorption of Congo red dyes. (b)Thermodynamic function graph (The concentration of Congo red dye was 120 mg/L ,PSD-NH_2 dosage of 5 mg, pH 3.5, time of 120 min and volume 10 mL)

Table 4

Thermodynamic parameters of Congo red on PSD-NH_2 microspheres

T(K)	ΔG^0 (kJ mol^{-1})	ΔH^0 (kJ mol^{-1})	ΔS^0 (kJ mol-1 K^{-1})
293.15	-2.629		
298.15	-3.164		
303.15	-3.699	28.722	0.107
313.15	-4.769		
323.15	-5.839		
333.15	-6.909		

Adsorption Mechanism. There are many factors that play a decisive role in the phenomenon of dye adsorption, such as structural properties, dye structure, surface chemistry of adsorbent and the relationship between specific interaction of adsorbent and adsorbent molecules.[47] There are $–SO^{3-}$ and $–NH_2$ groups in the Congo red molecular structure. When the pH decreases, $-NH_2$ on the surface of the adsorbent and on the Congo red molecule are protonated to $–NH^{3+}$ and the electrostatic attraction between

the two is weakened, resulting in a decrease in the adsorption capacity. It can be seen from Figure 3, under suitable pH conditions, some Congo red molecules flocculate on the surface of the adsorbent, indicating that a certain amount of flocculation occurs while adsorption.[48] The adsorption process may include a certain adsorption bridging effect. Congo red molecules form molecules interaction force. Congo red with the largest molecular size is linear, and has a high negative charge and largest number of aromatic rings. Therefore, the selective adsorption mechanism for Congo red dye can be summarized as intermolecular electrostatic interaction, hydrogen bond between PSD-NH_2 microspheres adsorbed on the surface and Congo red, π-π and C-H…π stacking and other molecular forces,[49] such as Figure 9 shows.

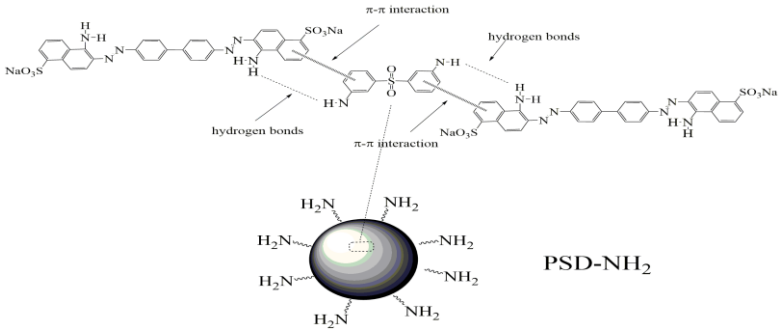

Figure 9. Schematic diagram of the possible interactions between PSD-NH_2 and Congo red: electrostatic attraction and π-π interaction

EXPERIMENTS

Starting Materials. Hexachlorocyclotriphosphazene (HCCP) and triethylamine (TEA) were purchased from Shanghai Aladdin Biochemical Technology Co., Ltd. 3,3'-Sulfonyldianiline was obtained from Shanghai Haohong Biomedical Technology Co., Ltd. Anhydrous ethanol and Congo red (CR) dyes were obtained from Hebei Industrial Analytical Reagent Factory and Shanghai Maclean Biochemical Technology Co., Ltd. Respectively all chemical reagents were analytical pure and were used directly .

Synthesis of amino polyphosphazene (PSD-NH_2) microspheres. Typically, 2.1429 g (6.1637 mmol) of 3,3'-sulfonyldianiline (MW: 248.30) and 0.7572 g (3.0495 mmol) of HCCP (MW: 347.66) were dissolved in 100 mL of MeCN, then the mixed solution was poured into a three-necked flask, shaken to dissolving it completely and 3 mL of triethylamine (TEA) was added to the solution dropwise. Use nitrogen as the protective gas, set the reaction temperature to 65 °C, and place the three-necked flask in an ultrasonic instrument (200 W, 40 KHz) for 12 h, then the reaction system was transferred to an oil bath and the reaction mixture stir for 12 h, the process is repeated twice (Ultrasound and heating). After the reaction was over, the products were centrifuged in a centrifuge machine (4000 r/min) for 5 min, and the separated precipitate was washed 3 times with absolute ethanol and deionized water, respectively. At last, the

washed product was dried in an oven (65 ºC) for 24 h to obtain pale yellow solid PSD-NH_2 microspheres.[50] The synthesis of PSD-NH_2 microspheres was shown in Figure 10.

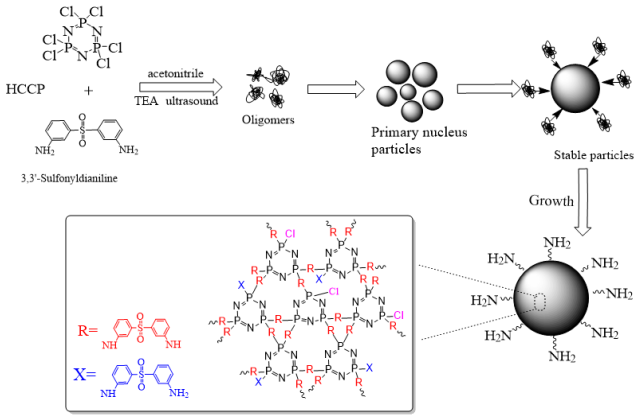

Figure 10. The synthetic schematic diagram of PSD-NH_2 microspheres

Characterization. On the Shimadzu (Japan) IR Prestige-21 infrared spectrometer, KBr solid tablets was used to measure the infrared spectra in the range of 400-4000 cm^{-1}, and the material was initially qualitatively analyzed. Observation of the size and morphology of PSD-NH_2 microspheres with S-3400N scanning electron microscope (SEM). The phase analysis of the sample was carried out with D8Advance, Bruker AXS, Germany an X-ray diffraction spectrometer, Cu-Kα radiation was selected, and the scanning rate was 8°/min. Elemental analysis of PSD-NH_2 microspheres were performed by XPS (Escalab 250 Xi). Before starting the adsorption experiment, different concentrations of Congo red (20-160 mg/L) were prepared, and the Congo red solution of different concentrations was measured to obtain the corresponding absorbance. The wavelength of Congo red under different pH values was tested, and the maximum characteristic absorption wavelength (499 nm) (pH=5.0-12.0), the value under the condition of 580 nm (pH=2.0-5.0) [pHS-2C pH meter]((Shanghai Dazhong Analytical Instruments Co., Ltd.) were selected. The equation origin was obtained by linear extrapolation of the standard curve of Congo red.

ACKNOWLEDGEMENTS

The authors gratefully acknowledge support from the National Natural Science Foundation of China (51803088), Scientific Research Fund of Hunan Education Department (17C1360).

REFERENCES AND NOTES

1. G. Crini, *Bioresour. Technol.*, 2006, **97**, 1061.
2. S. H. Huo and X. P. Yan, *J. Mater. Chem.*, 2012, **22**, 7449.
3. Z. P. Qi, J. M. Yang, Y. S. Kang, F. Guo, and W. Y. Sun, *Dalton Trans.*, 2016, **45**, 8753.

4. G. L. Huang, Y. Y. Sun, C. C. Zhao, Y. F. Zhao, Z. Y. Song, J. L. Chen, S. L. Ma, J. P. Du, and Z. G. Yin, *J. Colloid Interface Sci.*, 2017, **494**, 215.
5. W. K. Dong, Y. S. Lu, W. B. Wang, L. Zong, Y. F. Zhu, Y. R. Kang, and A. Q. Wang, *Microporous Mesoporous Mat.*, 2019, **27**, 267.
6. S. K. Low, M. C. Tan, and N. L. Chin, *Ultrason. Sonochem.*, 2018, **48**, 64.
7. J. Dasgupta, J. Sikder, S. Chakraborty, S. Curcio, and E. Drioli, *J. Environ. Manage*., 2015, **147**, 55.
8. D. Hank, Z. Azi, S. A. Hocine, and O. Chaalal, *J. Ind. Eng. Chem.*, 2014, **20**, 2256.
9. S. S. Moghaddam, M. R. A. Moghaddam, and M. Arami. *J. Environ. Health Sci. Eng.*, 2010, **7**, 437.
10. H. Y. Zhao, Y. H. Li, D. S. Wang, and L. Zhao, *Eur. J. Inorg. Chem.*, 2018, **1145**.
11. Q. Liang, S. N. Cui, C. H. Liu, S. Xu, C. Yao, and Z. Y. Li, *J. Colloid Interface Sci.*, 2018, **524**, 379.
12. M. M. Martorell, H. F. Pajot, and L. I. C. de Figueroa, *J. Environ. Chem. Eng.*, 2017, **5**, 5987.
13. L. Zhang, L. Y. Tu, Y. Liang, Q. Chen, Z. S. Li, C. H. Li, Z. H. Wang, and W. Li, *RSC Adv.*, 2018, **8**, 42280.
14. X. B. Luo, Y. C. Zhan, Y. N. Huang, L. X. Yang, X. M. Tu, and S. L. Luo, *J. Hazard. Mater.*, 2011, **187**, 274.
15. S. T. Khankhasaeva, E. T. Dashinamzhilova, A. L.Bardamova, and O. Z.Ayurova, *Russ. J. Appl. Chem.*, 2019, **92**, 282.
16. S. B. Wang and Y. L. Peng, *Chem. Eng. J.*, 2010, **156**, 11.
17. J. L. Gong, B. Wang, G. M. Zeng, C. P. Yang, C. G. Niu, Q. Y. Niu, W. J. Zhou, and Y. Liang, *J. Hazard. Mater.*, 2009, **164**, 1517.
18. K. W. Jung, S. Y. Lee, J. W. Choi, and Y. J. Lee, *Chem. Eng. J.*, 2019, **369**, 529.
19. S. G. P. Singaravel and R. Hashaikeh, *J. Mater. Sci.*, 2016, **51**, 1133.
20. J. W. Fu, Q. Q. Xin, X. C. Wu, Z. H. Chen, Y. Yan, S. J. Liu, M. H. Wang, and Q. Xu, *J. Colloid Interface Sci.*, 2016, **461**, 292.
21. M. Shanehsaz, S. Seidi, Y. Ghorbani, and S. M. R. Shoja, *Spectrochim. Acta A Mol. Biomol. Spectrosc.*, 2015, **149**, 481.
22. J. Qin, F. X. Qiu, X. S. Rong, J. Yan, H. Zhao, and D. Y. Yang, *Toxicol. Environ. Chem.*, 2014, **96**, 849.
23. S. S. Li, X. Z. Kong, X. B. Jiang, and X. L. Zhu, *Chin. Chem. Lett.*, 2013, **24**, 287.
24. H. R. Allcock, *Curr. Opin. Solid State Mater. Sci.*, 2006, **10**, 231.
25. L. Hu, A. Q. Zhang, Y. Yu, Z. Zheng, S. X. Du, and X. J. Cheng, *Iran. Polym. J.*, 2014, **23**, 689.
26. P. Zhang, X. Huang, J. Fu, Y. Huang, Y. Zhu, and X. Tang, *Macromol. Chem. Phys.*, 2009, **210**, 792.
27. X. Y. Huang, J. P. Bin, H. T. Bu, G. B. Jiang, and M. H. Zeng, *Carbohydr. Polym.*, 2011, **84**, 1350.

28. R. K. Voznicova, J. Taraba, J. Prihoda, and M. Alberti, *Polyhedron*, 2008, **27**, 2077.
29. J. Kohler, S. Kuhl, H. Keul, M. Moller, and A. Pich, *J. Polym. Sci. Pol. Chem.*, 2014, **52**, 527.
30. L. Q. Jin, W. G. Li, Q. H. Xu, and Q. C. Sun, *Cellulose*, 2015, **22**, 2443.
31. Z. K. Li, G. H. Wang, W. J. Ren, A. Q. Zhang, L. An, and Y. S. Tian, *J. Mater. Sci.*, 2016, **51**, 4096.
32. Z. L. Yang, K. Y. Fu, J. Yu, and X. Y. Liu, *J. Inorg. Organomet. Polym. Mater.*, 2019, **29**, 59.
33. R. Jain and S. Sikarwar, *Desalin. Water Treat.*, 2014, **52**, 7400.
34. G. Vijayakumar, M. Dharmendirakumar, S. Renganathan, S. Sivanesan, G. Baskar, and K. P. Elango, *Clean-Soil Air Water*, 2009, **37**, 355.
35. L. Torkian, B. G. Ashtiani, E. Amereh, and N. Mohammadi, *Desalin. Water Treat.*, 2012, **44**, 118.
36. J. W. Fu, Z. H. Chen, X. C. Wu, M. H. Wang, X. Z. Wang, J. H. Zhang, J. A. Zhang, and Q. Xu, *Chem. Eng. J.*, 2015, **281**, 42.
37. J. W. Fu, J. H. Zhu, Z. W. Wang, Y. H. Wang, S. M. Wang, R. Q. Yan, and Q. Xu, *J. Colloid Interface Sci.*, 2019, **542**, 123.
38. R. Q. Long and R. T. Yang, *J. Am. Chem. Soc.*, 2001, **123**, 2058.
39. Y. Li, A. Meas, S. D. Shan, R. Q. Yang, and X. K. Gai, *Bioresour. Technol.*, 2016, **207**, 379.
40. R. R. Shan, L. G. Yan, Y. M. Yang, K. Yang, S. J. Yu, H. Q. Yu, B. C. Zhu, and B. Du, *J. Ind. Eng. Chem.*, 2015, **21**, 561.
41. H. Shayesteh, A. Rahbar-Kelishami, and R. Norouzbeigi, *J. Mol. Liq.*, 2016, **221**, 1.
42. E. N. Seyahmazegi, R. Mohammad-Rezaei, and H. Razmi, *Chem. Eng. Res. Des.*, 2016, **109**, 824.
43. X. Q. Zhang, Y. F. Gao, H. T. Liu, and Z. L. Liu, *CrystEngComm.*, 2015, **17**, 6037.
44. S. Chatterjee, S. Chatterjee, B. P. Chatterjee, and A. K. Guha, *Colloids Surf. A Physicochem. Eng. Asp.*, 2007, **299**, 146.
45. A. A. El-Zahhar, N. S. Awwad, and E. E. El-Katori, *J. Mol. Liq.*, 2014, **199**, 454.
46. A. M. M. Vargas, A. L. Cazetta, A. C. Martins, J. C. G. Moraes, E. E. Garcia, G. F. Gauze, W. F. Costa, and V. C. Almeida, *Chem. Eng. J.*, 2012, **181**, 243.
47. H. Chaudhuri, S. Dash, and A. Sarkar, *New J. Chem.*, 2016, **40**, 3622.
48. Q. Liu, C. Han, W. Sun, J. Yang, and Y. Zhou, *Stud. Surf. Sci. Catal*, 2003, **146**, 177.
49. Z. Liu, H. S. Wang, C. Liu, Y. J. Jiang, G. Yu, X. D. Mu, and X. Y. Wang, *Chem. Commun.*, 2012, **48**, 7350.
50. J. M. Zou, K. F. Liao, L. Xiang, M. W. Liu, F. Xie, X. L. Liu, J. L. Yu, X. N. An, and Y. F. Wang, *J. Inorg. Organomet. Polym. Mater.*, 2020, **30**, 976.